CONF-9705 03 -- 70

BNL-63974

MAGNETIC MEASUREMENTS ON AN IN-VACUUM UNDULATOR FOR THE NSLS X-RAY RING*

G. Rakowsky, J.J. Aspenleiter, W.S. Graves, L. Solomon and P.M. Stefan
NSLS, Brookhaven National Laboratory, P.O. Box 5000, Upton, NY 11973-5000, USA

RECEIVED
JUN 2 4 1997
OSTI

Abstract

Magnetic measurements have been performed on the In-Vacuum Undulator (IVUN), built jointly by BNL and SPring-8 for the NSLS X-Ray Ring. The IVUN magnet has a Halbach-type, pure-permanent magnet structure with a period of 11 mm and a minimum gap of 2 mm. Results of magnetic measurements utilizing Hall probe, moving wire and pulsed wire techniques will be presented and compared.

INTRODUCTION

A short-period, In-Vacuum UNdulator (IVUN) is being developed in a collaboration between Spring-8 and NSLS for installation in the NSLS X-Ray Ring [1]. This magnet builds on experience gained in the successful development and operation of the in-vacuum undulator for the KEK Accumulator Ring [2] and the Prototype Small-Gap Undulator (PSGU)] in the NSLS X-Ray Ring.[3]. Studies with the PSGU have demonstrated minimal beam lifetime reduction in the X-Ray ring with apertures as small as 3mm in low-beta straight sections. With an in-vacuum device, the magnet array itself, rather than the vacuum chamber, can be the limiting aperture. The IVUN design explores this new parameter regime. Details of the IVUN design are presented by Tanabe [4] elsewhere in these Proceedings. Installation of IVUN in the NSLS X-Ray Ring is scheduled for May, 1997.

The magnet arrays were assembled, mapped, trimmed, vacuum baked and remeasured at SPring-8 before shipment to NSLS. The magnet array support structure and vacuum chamber were designed and built at NSLS. Upon arrival at the NSLS, the magnet arrays were mounted to the support structure and gap drive system for magnetic measurements. This paper reports the results of these measurements.

1 DESIGN HIGHLIGHTS

The IVUN magnet design employs a pure-permanent magnet, Halbach-type structure with four blocks per period. The arrays are 30.5 periods long with +3/4, -1/4 type (displacement-free) terminations. With a design gap of 3.3 mm and a period of 11 mm, the IVUN magnet achieves a peak field of 0.7 Tesla and a K value of 0.72., The design fundamental peak is at 4.6 keV

(2.7Å) for the X-Ray Ring energy of 2.584 GeV. High-temperature neodymium-iron-boron magnets (Sumitomo NEOMAX 32EH) were used, allowing bakeout at up to 125°C.

The magnet arrays, with their water-cooled backing beams, are each supported by a single post via bellows through the rectangular vacuum chamber flanges. The variable-gap drive and support structure are nearly identical to that of the PSGU. The gap is adjustable from 10 mm down to 1 mm, but will be limited to 2 mm by controls, limit switches and hard stops.

Electron beam image currents are carried from the Conflat end flanges to the gap region by flexible transitions and bellows liners of a design developed for the PSGU. In the gap region the current will be carried by high-purity, annealed nickel foil strips, 0.1 mm thick, laid directly on the magnet pole surfaces.

3 MAGNETIC MEASUREMENTS

The magnetic measurements at NSLS had a three-fold objective: (1) to verify that the magnet assembly had not been damaged in transit, (2) to perform measurements complementary to those already done at Spring-8, and (3) to measure the effect of the nickel image-current continuity sheets on magnet performance.

Visual inspection of the magnet arrays upon arrival at NSLS showed no damage in transit. However, soon after, a magnet broke spontaneously. This raised concerns about possible additional magnet failures, particularly since a magnet had also broken at Spring-8 during vacuum-compatibility bakeout testing. A magnet breakage in an in-vacuum device such as IVUN is much more serious than in a conventional insertion device. Therefore, in parallel with the magnetic measurements, a detailed modeling study was undertaken to analyze the forces and stresses involved. As a result, each pair of magnet block retaining clips was systematically loosened and retorqued, so as to limit the maximum stress in the NdFeB to 50% of its tensile strength. As a further precaution, the reassembled magnet was then cycled over 100 times between 9.5 mm and 2 mm gap, without any further magnet failures.

3.1 Hall Probe Measurements

Hall probe measurement of the IVUN magnet was done on a granite mapper using a miniature Group3 transverse

MASTER

Hall probe with built-in temperature correction. The probe's response was calibrated against NMR probes in a standard dipole magnet. A fifth-order polynomial was used to fit the Hall probe voltage vs. field data. Only the vertical (y) component of B was mapped with the Hall probe system.

Field maps were taken in the midplane (Y=0) at X=0, ±2 and ±4 mm, at the nominal 3.3 mm gap. On-axis field maps [X=0, Y=0) were taken at several gaps between 3.3 and 9.5 mm. To help correlate certain trajectory features with either the upper or lower magnet array, off-midplane scans were also taken at the 9.5 mm gap, with the probe at X=0 and Y=±3.1 mm, i.e., at 1.65 mm from each array, the same distance as in the midplane scan at 3.3 mm gap.

First integrals of these Hall probe scans show that the integrated dipole varies from about 30 to 70 gauss-cm for -2mm<X<+2mm. The quadrupole error is about 100 gauss, exceeding the design goal of 10 gauss. These results differ significantly from Tanabe's data, which will be discussed in the following paragraph.

The second integral of the field is proportional to the e-beam trajectory and reveals the location of non-canceling field errors. The on-axis trajectory, calculated from Hall probe data, is shown in Figure 1 and is in good agreement with Tanabe's result. The off-axis trajectories (not shown) show local dipole errors which vary with X, and which suggest that various magnet blocks may have large multipole errors. Comparison of off-axis trajectories with Tanabe's data show local deviations in the region of the block replaced at NSLS. This suggests that the replacement block may have significantly different multipoles from the broken one, which would account for the discrepancy in integrated multipoles reported above.
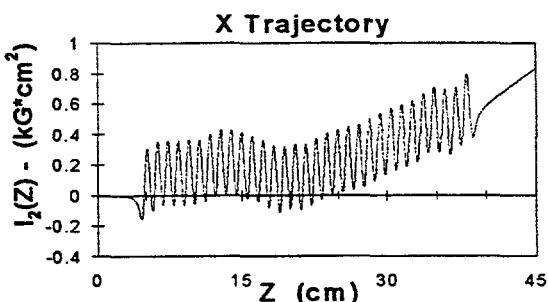

Figure 1. IVUN on-axis trajectory at 3.3 mm gap.

3.2 Nickel Continuity Sheets.

The effect of the nickel continuity sheets was measured by mapping the field with and without the foils at a gap of 3.3 mm. As expected, field amplitude decreased due to shunting of flux from pole to neighboring pole. At a field amplitude of about 0.7 Tesla, the decrease in peak field varied between 20 and 30 gauss, with larger deviations near the zero crossings. Because the effect is

symmetric, the trajectory plots and the phase error plots appear virtually identical, so there should be no degradation of performance.

3.3 Moving-Wire Measurements

The small gap led us to choose a moving wire integrator, similar to a design reported by Zangrando and Walker, [6] to measure integrated fields. The wire was a 43-strand Litz cable formed into a loop, with the strands connected in series. The leg of the loop passing through the undulator is stretched between supports mounted on motorized translation stages. Integrated dipole profiles are obtained by measuring the voltage induced in the loop with an integrating voltmeter, as the wire is translated through the magnet in increments of DX. Due to random drift in the integrating voltmeter, voltage readings were averaged over many repetitions to achieve adequate signal-to-noise. As with the Hall probe, only normal (By) field integrals were measured, due to the restricted gap.
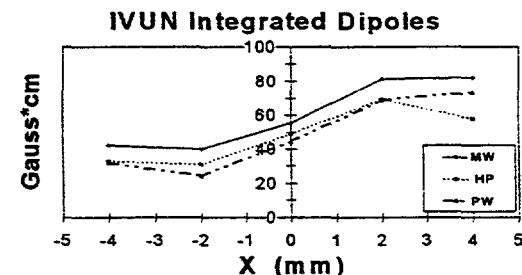

Figure 2. Integrated dipoles in IVUN from Hall probe (HP), moving wire (MW) and pulsed wire (PW) data.

Integrated dipoles were measured in the midplane (Y=0) at 2 mm intervals from -4mm to +4mm, at several gaps, with DX=2mm. Figure 2 compares the integrated dipole profiles at 3.3mm gap obtained from the moving wire with those computed by numerical integration of Hall probe data. These profiles agree qualitatively and indicate a strong quadrupole and octupole.

3.4 Pulsed Wire Measurements

The pulsed wire bench is modeled after the Los Alamos design developed by Warren and Fortgang [7], with the addition of viscous damping. Its main advantage is rapid visualization of both X and Y trajectories. In this case, it was our only means of measuring the Y trajectory.
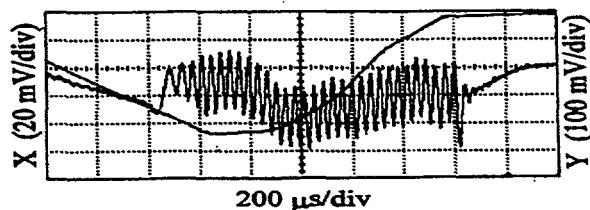

Figure 3. X and Y trajectories from pulsed wire.

DISCLAIMER

Portions of this document may be illegible in electronic image products. Images are produced from the best available original document.

DISCLAIMER

Figure 3 shows a "snapshot" of the on-axis X and Y trajectories in IVUN at a gap of 3.3mm. The X trajectory agrees quite well with the trajectory shown in Figure 1, both in terms of the distinctive features discussed earlier, and in terms of the integrated dipole, (computed graphically from the entry and exit trajectory angles.) The distortion observed at the ends of the sinusoidal waveform is due to dispersive properties of the BeCu wire.

The Y trajectory exhibits a peak deviation of about 2.3 mm, equivalent to 9 wiggle amplitudes. This large trajectory error undoubtedly resulted from optimizing only the X trajectory, without benefit of an on-line, Y trajectory diagnostic. The Y trajectory shows distinct kinks which point to localized sources of Bx fields. Integrated dipoles calculated graphically from exit and entry trajectory angles are also in good agreement with those obtained from Hall probe scans and moving wire measurements (Figure 2). The Y trajectories also exhibit variation with off-axis position, indicating the presence of significant skew multipoles.
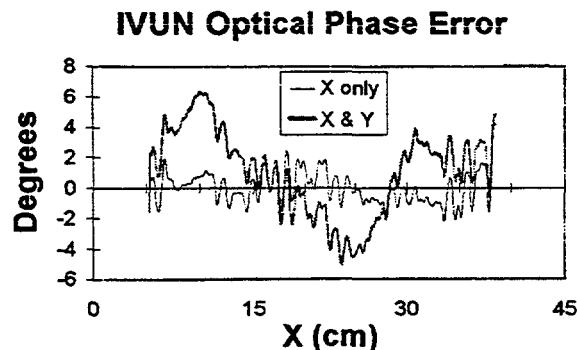
IVUN Optical Phase Error

Figure 4. Optical phase error due to (a) X trajectory only, and (b) both X and Y trajectory components.

3.5 Phase Shake Analysis

Optical phase error is an excellent measure of undulator quality since it is strongly correlated to loss of spectral brightness.[5] It is calculated by integrating the difference between the path length along the actual trajectory and a best-fit sinusoidal trajectory, expressed in degrees at the fundamental optical wavelength. Phase error calculated from our on-axis By field maps is shown by the "X only" curve in Figure 4. It shows rms phase shake of less than 2 degrees, predicting excellent spectral performance. Tanabe's data gives similar phase error results. However, phase error is also affected by Y trajectory errors due to Bx. The "X+Y" curve shows the phase error when both By and Bx are taking into account. As can be seen, the phase excursions have increased to $\pm$ 5°. The actual spectral brightness will therefore be lower than would be expected due to phase shake from X motion alone.

The phase error plot reveals mechanical alignment errors, particularly gap taper. This produces a field taper and results in a "chirp" in the resonant wavelength. Its effect on the optical spectrum is to smear the spectral lines. The presence of taper is revealed by a parabolic phase profile. For IVUN, a gap taper error of only 25 µm (0.001 in) resulted in a noticeable chirp of several degrees. This level of precision is just below the threshold of standard optical survey instruments, so the phase error plot becomes the best remaining diagnostic of magnet array alignment.

4 CONCLUSIONS

Magnetic field measurements on the IVUN undulator have been completed at NSLS. The Hall probe, moving wire and pulsed wire techniques proved to be mutually complimentary and the three sets of measurements are in good agreement. Intercomparison with measurements done earlier on this device at Spring-8 show generally good agreement in the X trajectories, except at the location where a broken magnet was replaced. Disagreement in multipole measurements can be attributed to differences in multipole characteristics of the replacement magnet from the broken one. Using the pulsed wire bench as an on-line diagnostic, it should be straightforward to find a better replacement magnet and also to retrim IVUN to minimize the Y trajectory errors and integrated multipoles.

5 ACKNOWLEDGEMENTS

REFERENCES

[1] P. Stefan, et al., 'Insertion Device Development in the X13 Straight of the NSLS X-Ray Ring', these Proceedings.

[2] S. Yamamoto et al., Rev. Sci. Instr., 63 (1), p.400, (1992).

[3] P.M. Stefan et al., Proc. 1995 Part. Accel. Conf., Dallas, TX, p.2435, (1995).

[4] T. Tanabe, et al., 'Development of an In-Vacuum Minipole Undulator', these Proceedings.

[5] B.L. Bobbs et al., Nucl. Instr. and Meth., A296, p.574, (1990).

[6] D. Zangrando and R.P. Walker, Nucl. Instr. and Meth., A376, p.275, (1996).

[7] R.Warren and C. Fortgang, Nucl. Instr. and Meth., A341, p.444, (1994).